University College of Takestan

Available online at http://UCTjournals.com

UCT Journal of Research in Science ,Engineering and Technology

UCT . J. Resea. Scien. Engineer.Techno.(UJRSET)

18-25 (2015)

Volume 3,Issue1

ISSN:2382-977X

The Mitigation of the Effect of Impulsive Noise in OFDM-PLC Systems

Mohammad Reza Ahadiat[*,1], Paeiz Azmi[2], Afrooz Haghbin[1]

[1]*Department of Electrical Engineering , Science and Research Branch, Islamic Azad University, Tehran, Iran*

[2]*Department of Electrical and Computer Engineering, Tarbiat Modares University, Tehran, Iran*

*Corresponding author's E-mail: m.ahadiat@srbiau.ac.ir

ABSTRACT

This paper proposes an new iterative method to recover the signals corrupted by impulsive noise in MIMO-OFDM systems over In-home PLC. In this iterative technique, preliminary decisions are made to get the impulsive noise detection algorithm for finding the locations and amplitudes of the impulses, and then signal estimation block for approximation the signals for two-branch 2*2 MIMO-OFDM at the receiver. In each iteration, this signals approximation are used to improve the noise estimate. After impulsive noise detection, an comparison - decision algorithm is employed to compare two noises estimated, and decision for cancel impulsive noise and improve Mitigation of the impulsive noise algorithm. This method use an adaptive threshold and soft decision to estimating and canceling the impulsive noises. Then, by using ML detection, an approximation of signal is obtained. As this impulsive noise detection , comparison - decision and ML detection loop continues, we get better approximates of the signal. The algorithm is analyzed and verified by computer simulations. A comparison between the performance of the different systems is presented and discussed. The Simulation results confirm the robustness of performance of the proposed algorithm.

Original Article:

Received 22 Sep. 2014
Accepted 25 Nov. 2014
Published 30 Mar. 2015

Keywords:
MIMO-OFDM, Impulsive Noise, iterative method, Power Line Communication

1. Introduction

The PLC (Power Line Communication) technology uses a power lines for its data communication. PLC networks can be divided into in-home network and out-home according to their applications. The applications of PLC in-home network have been increasing recently due to the development of HomePlug power line Alliance, which has published its standard, HomePlug Specification [1]. Digital communication systems over power line channel suffer from several disturbances. Such the disturbances are composed of colored Gaussian noise, impulsive noise, channel interference, frequency selective fading, attenuation, and so on[2,3] .

OFDM(Orthogonal Frequency Division Multiplexing) modulation schemes is a promising technique being used for bandwidth efficient communication over the PLC, Full capacity of the channel, high-speed data services broadband, Reduce the complexity equalization, its capacity to minimize ISI, and powerful in impulsive noise environments. It is also a strong candidate as a modulation scheme the performs better than single-carrier and spread spectrum modulation methods. OFDM minimizes the effects of multipath and provides high robustness against selective fading. In PLC, the reliability of transmission is strongly influenced by the non-Gaussian impulsive noise. In OFDM, the IDFT is used for modulating a block of N information symbols on N subcarriers[4]. The time duration of an OFDM symbol is N times larger than that of a single carrier system. This longer duration of OFDM symbol provide an advantage that the impulsive noise energy is spread among the N subcarriers due to the IDFT operation. This spreading causes less interference over all N subcarriers[5]. However, when the impulsive noise energy exceeds a certain threshold, a significant performance loss can occur due to the higher level of interference at each subcarrier[6]. It was shown in [7] that impulsive noise leads to an enormous loss in the capacity, as well as in the error rate performance.

Current high speed PLC technologies such as Homplug AV uses as Single-input Single-output (SISI) communication mode and provides usable application level throughputs on typical PLC channels of about 100 Mbps. Today's in-home power line channel for 3-wire installations (phase, neutral and protective earth) basically allow more feeding and receiving possibilities, which is the precondition to apply MIMO and Alamouti coding methods[8]. In [9] the suitability of MIMO for in-home PLC has been investigated. It has been shown that MIMO can significantly increase the bit rate. Typically it is more than doubled compare to today's SISO systems. Alamouti scheme is considered to be the best choice of different MIMO schemes in the PLC environment. The advantages of the MIMO-PLC system mainly lies in namely increased channel capacity and reduced BER[10]. MIMO techniques in combination with orthogonal frequency-division multiplexing (MIMO-OFDM) have been identified as a promising approach for high spectral efficiency wideband systems.

Different approaches for impulse noise suppression are proposed in literature. In this paper, we discuss mitigation of Effect of Impulsive Noise from a signal for MIMO (2*2) channel by Alamouti scheme in OFDM-based systems over In-home Power Line Channels. The signal is first converted to digital symbol. The serial data stream of the source is mapped to data symbols with employing the signal constellation scheme of 16 quadrature amplitude modulation(16-QAM). Complex symbols of each transmit path are then OFDM

modulated, Alamouti coding and sent via the two transmit paths over MIMO-PLC channel. On receiving side, the signals of two receiving ports are in a first step OFDM demodulated. Then symbols are ZF equalized. The resulting vector R_i is obtained for each path. The symbols of vector R_i consist of original symbols and noises. At the beginning of the iterative method, the initial detection of the impulsive noise locations is performed. adaptive threshold technique similar to radar's Constant False Alarm Rate (CFAR) detector[11] are used to detection. Then comparison-decision algorithm is used for improved data that have been corrupted by impulsive noise.

This algorithm has been used in a way to reduce the impact of impulsive noise and to compare two noises estimated and decision for cancel impulsive noise and improve mitigation of the impulsive noise algorithm. The result of comparison-decision algorithm is used to ML detection as signal estimation. As impulsive noise detection, comparison-decision and ML detection loop continues, we get better approximates of the signal.

2. SYSTEM MODEL

The general model of a PLC is depicted in Figure 1.

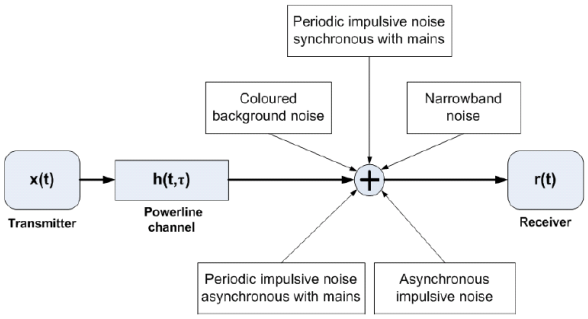

Figure 1. Noise on PLC

The $h(t,\tau)$ is channel impulse response and is represented by a channel filter and different noise components as depicted in Figure 1 can be expressed as background noise and impulsive noise[12].

2.1. BACKGROUND NOISE MODELING

The background noise can create disturbances in the frequency range 0-100 MHz [13]-[14]. The background noise Can be separated in Colored noise and Narrowband interference[12]. The background noise according to [15], can be modeled in the simple three-parameter model, where the noise is considered Gaussian with the power spectral density (PSD)

$$R_{n_b}(f) = a + b|f|^c \quad [\frac{dBm}{Hz}] \qquad (1)$$

where *f* is the frequency in MHz, and *a*, *b* and *c* are parameters derived from measurements. we obtain a worst case scenario by [*a*, *b*, *c*] =[-145, 53.23,-0.337], while we obtain a best case scenario with [*a*, *b*, *c*] = [-140, 38.75,-0.72]. The resulting PSDs are depicted in Figure 2.

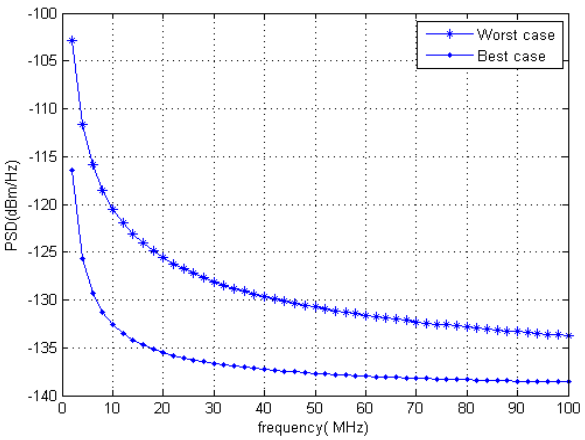

Figure 2. PSD for good and Bad background noise.

2.2. IMPULSIVE NOISE MODELING

The impulsive noise Can be separated in Periodic impulsive noise synchronous with the mains frequency, Periodic impulsive noise asynchronous with the mains frequency and Aperiodic impulsive noise[12],[16].

Therefore, the overall noise can be written as

$$\eta(t) = n_b(t) + n_{imp}(t) \qquad (2)$$

where $n_b(t)$ denotes the background noise, while $n_{imp}(t)$ denotes the impulsive noise. The impulsive noise can be modeled with an arrival process. This process is specified by the statistics of the impulse amplitude A_{imp}, interarrival time t_{iat}, and duration t_{wid}. Most of the literature focuses on the statistics of the amplitude, as the Middleton's classification of electromagnetic interference [17] and the two-term Gaussian mixture [18] model. The temporal characteristics have been modeled via Markov chains in[12], Bernoulli process in [19] and curve fitting tools from experimental measurements in [15].

A relatively simple model which incorporates background noise and impulsive noise based on the Poisson-Gaussian model is known as Midlenton's class-A impulsive

In the Middleton's model[17], the noise is categorized into three different types A, B and C. Because Midlenton's class-A impulsive noise model is more accurate and also meets all the basic requirements in modeling the real impulsive noise, this model has been used widely in performance analysis of PLC systems. This thesis also relies on Midlenton's class-A to model impulsive noise and design communications systems over power lines. Midelenton's class-A model uses the Poisson-Gaussian model to represent the background noise and impulsive noise. The occurrence probability of impulsive noise is modeled by a Poisson random process with the probability of having m impulsive noise events in a time interval T given by

$$P = \frac{(\lambda T)^m e^{-\lambda T}}{m!} \qquad (3)$$

The amplitudes of both background and impulsive noise are modeled by Gaussian random processes. Let $A = \lambda T$ and call it the impulsive index. Then the probability density function of Midlenton's class-A impulsive noise is written as

$$p_A(n) = \sum_{m=0}^{\infty} \frac{e^{-A} A^m}{m!} \cdot \frac{1}{\sqrt{2\pi\sigma_m^2}} \exp\left(-\frac{n^2}{2\sigma_m^2}\right) \qquad (4)$$

$$\sigma_m^2 = \left(\frac{\left(\frac{m}{A}\right) + \Gamma}{1+\Gamma}\right).\sigma^2$$

$$A \in [10^{-2}, 1], \Gamma \in [10^{-6}, 1]$$

where σ_m^2 is the mth impulsive power, *A* is impulsive index, σ^2 is total noise power (including the powers of impulsive noise and Gaussian background noise), and $\Gamma = \frac{\sigma_G^2}{\sigma_i^2}$ is Gaussian-to-impulsive noise power ratio (GIR) with σ_G^2 and σ_i^2 are the powers of Gaussian and impulsive noise, respectively. When A is increased, the impulsiveness reduces and the noise comes closer to Gaussian noise. Equation (4) also shows that sources of impulsive noise have a Poisson distribution, and each impulsive noise source generates a characteristic Gaussian noise with a different variance. A good approximation of Equation(4), is obtained by cutting off the cumulative sum after the third term [18]. The effects of impulsive parameters A and are illustrated in Figure 3 and Figure 4.

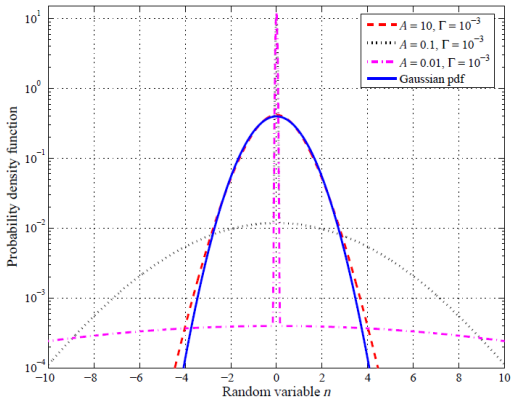

Figure 3. Pdf of the impulsive noise with different values of impulsive index A.

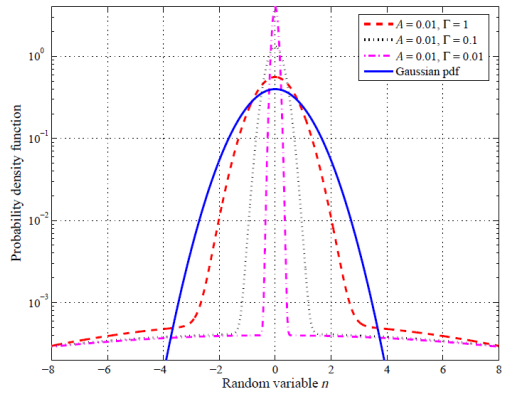

Figure 4. Pdf of the impulsive noise with different values of GIR Γ

Figure 5 also illustrate the effects of the impulsive noise parameters A and Γ to the amplitude distribution of class-A impulsive noise. Again, it can be seen that if A or Γ increases, the amplitude distribution of impulsive noise comes closer to that of Gaussian noise.

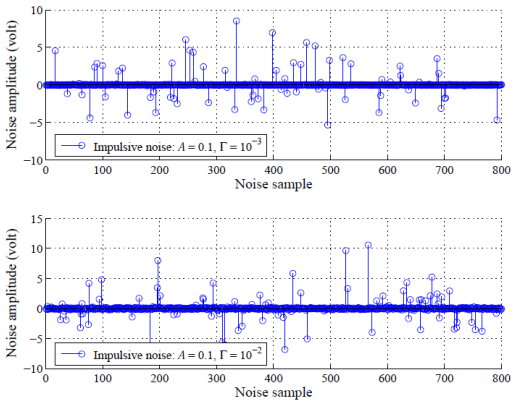

Figure 5. Examples of impulsive noise with A=0.1 and two different values of Γ.

2.3. MIMO-PLC CHANNEL MODELING

In this paper, MIMO-PLC system which considers the coupling effects among conductors Can be modeled by Zimmermann and Dostert model[20] where the MIMO-PLC model is considered with the channel transfer function (CTF) [20]:

$$H(f) = B\sum_{p=1}^{N_p} g_p(f).e^{-\alpha(f)d_p}.e^{-j\left(\frac{2\pi f d_p}{v_d}\right)}$$

(5)

$$\alpha(f) = \text{Real}\{= \alpha + j\beta = \sqrt{(R' + j\omega L')(G' + j\omega C')}\}$$

where N_p , B , $|g_p| \leq 1$, $\tau_p = \frac{d_p}{v_d}$, d_p , $v_d = \frac{c}{\sqrt{\varepsilon_r}}$, ε_r , γ, α and β and are the total number of fading paths, normalization term, the transmission reflection factor for path p, the pth path propagation delay, the length of the pth path, the phase velocity with c speed of light, dielectric constant , the propagation constant, the attenuation constant and the phase constant, respectively. so we are only interested in the attenuation constant. The primary cable parameters L' (inductance per unit length) and C' (capacitance per unit length) can be estimated by the geometric dimensions and the material properties. The R' (resistance per unit length) and G' (conductance per unit length) depend on frequency. The attenuation of a power line cable can be characterized by[21]

$$A(f, d_p) = e^{-\alpha(f)d_p} = e^{(a_0 + a_1 f^k)d_p}$$

(6)

The parameters a_0, a_1, K are chosen to adapt the model to a specific network. In this paper According to [22] a statistical model of the channel can be derived by considering the parameters in Equation (5) as random variables. The path lengths are assumed to be drawn from a Poisson arrival process with intensity Λ in m^{-1}. The reflection factors $g_p$are assumed to be real, independent, and uniformly or log-normally distributed. Finally, the parameters a_0, $a_1$and K are appropriately chosen to a fixed value[23].

All PLC available today use one transmitting and one receiving port for their communication. The signal is symmetrically fed and received between the live and neutral wire. In Iran, in-home installations consist of three wires, which offers additional feeding and receiving options. Figure 6 shows the PLC MIMO channel. Differential signaling between any two of the three wires lead to three different feeding possibilities: P (Phase or Live) to N (Neutral), P to PE (Protective Earth), and N to PE.

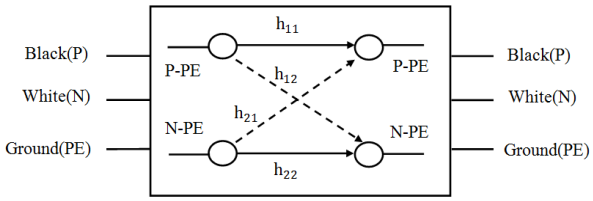

Figure 6. PLC MIMO channel.

According to Kirchhoff's rule the sum of the three input signals has to be zero. Therefore only two out of the three independent input ports can be used. On receiving side all three differential reception ports are available[8]. The coupling effects between conductors in the MIMO-PLC should be considered. The CTF In MIMO system for the ith transmit to the jth receive path (where i = 1, 2 and j = 1, 2) can be written as

$$H_{i,j}(f) = \sum_{p=1}^{N_p} B\, g_p(f).e^{-\alpha_{i,j}(f)d_p}.e^{-j2\pi f\tau_p}$$

(7)

Equation (7) can be extended to the overall transfer function matrix:

$$H_{MIMO} = \begin{bmatrix} H_{1,1}(f) & H_{1,2}(f) \\ H_{2,1}(f) & H_{2,2}(f) \end{bmatrix} \quad (8)$$

where $H_{i,j}$, $i = j$ indicate co-channels and $H_{i,j}$, $i \neq j$ indicate cross channels. The attenuation constant $\alpha_{i,j}$ in Equation (7) can be extracted from

$$\alpha_{i,j} = \text{real}\{\left(\sqrt{(R'' + j\omega L'').*(G'' + j\omega C'')}\right)_{i,j}\}$$

(9)

where the operator .* indicates the element-wise matrix multiplication. R'', L'', C'' and G'' correspond to transmission line

matrices[24], which represent the mutual interactions between conductors. The equivalent per-unit-length (p.u.l) parameter model [9] can be used to characterize the in-home transmission line, as shown in Figure 7.

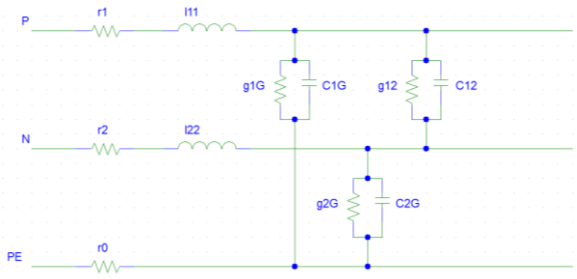

Figure 7. The equivalent per-unit-length parameter model for in-home plc.

The resistance matrix is

$$R'' = \begin{bmatrix} r_1 + r_0 & r_0 \\ r_0 & r_2 + r_0 \end{bmatrix} \quad (10)$$

where r_0, r_1 and r_2 are the ground resistance, the resistances for line P and the resistances for line N (which indicates line 1, line 2 in Figure 7) per unit length, respectively and computed as

$$r_1 = r_2 = \frac{1}{2}\sqrt{\frac{\pi f \mu_c}{\sigma_c}} \quad (11)$$

where μ_c, σ_c and f and are the permeability and conductivity of conducting material, the wave frequency and, respectively. The inductance matrix is

$$L'' = \begin{bmatrix} l_{11} & l_{12} \\ l_{21} & l_{22} \end{bmatrix} \quad (12)$$

where the l_{11} ,l_{22} are the self-inductances for line P, N per unit length and the l_{12} ,l_{21} are the mutual inductances. The computation for self-inductance per unit length is given as

$$l_{11} = l_{22} = \frac{\mu_0}{2\pi}\ln\frac{GMD}{GMR_L} \quad , GMD = D_{12} \quad (13)$$

Note that GMD, μ_0 and GMR_L are geometric mean distance, the permeability of dielectric material between conductors and geometric mean radian. The anti-diagonal terms in Equation(12) can be computed as $l_{12} = l_{21} = k\sqrt{L_{11}L_{22}}$. where k is called the coefficient of coupling ($0 \le k \le 1$). The capacitance matrix is

$$C'' = \begin{bmatrix} c_{11} & -c_{12} \\ -c_{21} & c_{22} \end{bmatrix} \quad (14)$$

where c_{11} and c_{22} are the self-capacitances for line P, N per unit length and given as $c_{11} = c_{1G} + c_{12}, c_{22} = c_{2G} + c_{21}$.and c_{PG}, c_{NG} (i.e., c_{1G}, or c_{2G}) are the capacitances between line P, N and ground (G), and given as

$$c_{1G} = \frac{2\pi\varepsilon_0}{\ln\frac{GMD}{GMR_C}} \quad (15)$$

$$c_m = 4\pi\varepsilon_0 (= -c_{12} = -c_{21})$$

where ε_0 and GMR_C are the permittivity of dielectric material between conductors and the actual conductor radius r. The conductance matrix is

$$G'' = \begin{bmatrix} g_{11} & -g_{12} \\ -g_{21} & g_{22} \end{bmatrix} \quad (16)$$

$$g_{1G} = 2\pi f c_{1G} \tan\delta \ , \ g_m (= -g_{12} = -g_{21})$$

where g_{11} and g_{22} are the self-conductances for line P, N per unit length and given as $g_{11} = g_{1G} + g_{12}, g_{22} = g_{2G} + g_{21}$.where g_{PG}, g_{PG}(i.e., g_{1G} or g_{2G}) are the conductances between line P, N and ground (G), δ is the skin depth of the conducting material. Performing the required mathematical operation in each element of the transmission parameter matrices to solve for the attenuation factor $\alpha_{i,j}$ in Equation (9), (i.e., $\alpha_{1,1} = \sqrt{(r_1 + r_0 + j\omega l_{11})(g_{11} + j\omega c_{11})}$,$\alpha_{1,2} = \sqrt{(r_0 + j\omega l_{12})(g_{12} - j\omega c_{12})}$), the channel matrix in Equation (10) can be obtained. [24]-[25].

2.4. OFDM SYSTEM MODELING

Figure 8 shows the block diagram of a MIMO OFDM system.

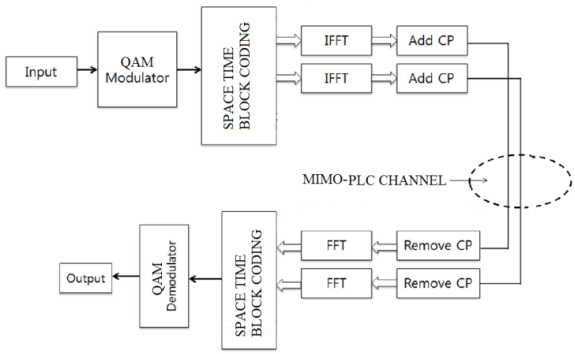

Figure 8. Block diagram of the proposed 2*2 MIMO-OFDM System.

In the transmitter side, input signal is first converted to digital symbol. The serial data stream of the source is mapped to data symbols with employing the signal constellation scheme of 16 quadrature amplitude modulation(16-QAM). Then, modulated symbols are fed to the space time block encoder [26]. Complex symbols of each transmit path are processed by OFDM modulated by an Inverse Fast Fourier Transform (IFFT) and a cyclic prefix (CP) insertion block. The symbols are then transmitted to the receiver via a 2*2 MIMO in-home power line channel, as shown in Figure 6. The receiver performs the reverse operation of the transmitter. The received signal is carried out by cyclic prefix removal, FFT operation.

3. THE PROPOSED METHOD

The symbols are received of 2*2 MIMO-PLC by Alamouti scheme in OFDM-based systems over In-home Power Line Channels. The received symbols in the first time slot, and by Assuming that the channel remains constant for the second time slot, the received symbols in the second time slot are

$$\begin{aligned} R_{11} &= H_{11}S_1 + H_{12}S_2 + N_{11} \\ R_{12} &= H_{21}S_1 + H_{22}S_2 + N_{12} \\ R_{21} &= -H_{11}S_2^* + H_{12}S_1^* + N_{21} \\ R_{22} &= -H_{21}S_2^* + H_{22}S_1^* + N_{22} \end{aligned} \quad (17)$$

The received symbols are equalized by zero forcing (ZF) equalization as shown in Figure 9.The received symbols consist of original symbols and noises, which can be computed as

$$R = HS + N \ , \tilde{S} = S + (H^H H)^{-1} H^H . N \quad (18)$$

$$\tilde{S}_1(m) = S(m) + E_1(m), \tilde{S}_2(m) = S(m) + E_2(m)$$

As depicted in Figure 9, successive detection and estimation of locations and amplitudes of impulsive noise are used to improve the quality of signal reconstruction[27]. In each Detection and Estimation step, the noise estimate improves using the signal estimated in the previous step. In the Impulsive noise detection block If amplitude of the impulses are large enough, corrupted samples could be differentiated from the neighboring samples. Detection in this block is based on the difference of the sample and the average of its neighbours. This is similar to the CFAR algorithm used in Radar [11]. The next step is deciding about a sample is noisy or not. This is

done by comparing each sample with the adaptive threshold. Then attenuate of each noisy sample by a factor between zero and one. This factor is depending on the certainty about the noisiness of the sample. This method is called soft decision and the attenuating factors are called the modulus. In each Detection and Estimation step, we obtain a new modulus. After impulsive noise detection algorithm, an comparison - decision algorithm is employed to compare two noises estimated and decision for cancel impulsive noise and improve Mitigation of the impulsive noise algorithm.

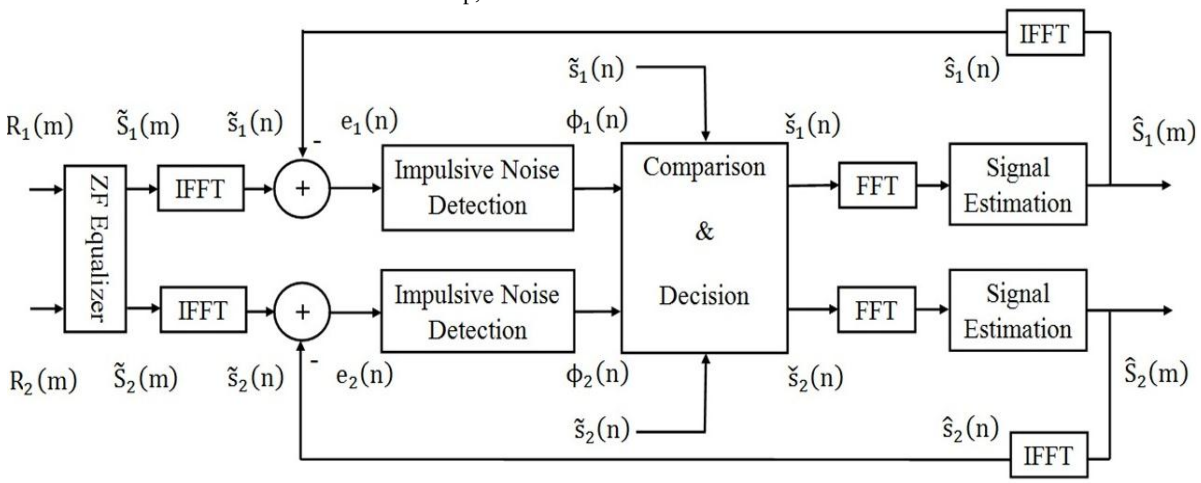

Figure 9. Block of the proposed method.

3.1. Impulsive Noise Detection

The threshold in impulsive noise detection block can either be adaptive or non-adaptive. The CFAR is an adaptive threshold method used in radar detectors based on Neyman-Pearson criterion[28]. In this paper we use a Censored Mean Level (CML) CFAR. The reason we use CML-CFAR is to reduce the probability that impulses involved in averaging when number of them are present in adjacent cells. In the kth order CML-CFAR of length $2n_c$, among the $2n_c$ adjacent cells, k of the smallest amplitudes are averaged and the other $2(n_c - k)$samples (which may contain impulsive noises) are ignored. In other words, if $|e[n_1]| \leq \cdots \leq |e[n_{2n_c}]|$ where $\{n_1, \ldots, n_{2n_c}\} = \{m - n_c, \ldots . . m + n_c\}$, we have:

$$\eta[m] = \frac{1}{k}\sum_{l=1}^{k}|e[n_l]| \quad (19)$$

The detection algorithm is not an error free process in the early Detection and Estimation steps, especially when the amplitudes of the impulsive noises are small compared to the Samples of the signal amplitudes. When the hard decision method is employed, the modulus is either zero or one at each sample. So that some samples are erased. One of the disadvantages of the soft method is its low convergence rate even when good estimates of the impulsive noise locations are available. To overcome this problem, **at** each stage of the Detection and Estimation we gradually change the soft decision to the hard decision. Simulation results for different modes suggested that the modulus function is as follows:

$$\emptyset(e[k], \eta[k]) = \exp(-\alpha|e[k] - \eta[k]|) \quad (20)$$

where $\hat{e}$, η and α are the estimated error, the threshold generated by CFAR [29] and the softness order of the soft decision, respectively. The suggested modulus function, the value $e[k] - \eta[k]$tends to zero, and then the α value is increased gradually through Detection and Estimation steps As the convergence rate increases.

3.2. Comparison and Decision Algorithm

The adaptive threshold and modulus function of two paths can be computed as

$$\eta_1[m] = \frac{1}{k}\sum_{l=1}^{k}|e_1[n_l]|\,; \eta_2[m] = \frac{1}{k}\sum_{l=1}^{k}|e_2[n_l]| \quad (21)$$

$$\emptyset_1(n) = e^{-\alpha|e_1(n)-\eta_1(n)|}; \emptyset_2(n) = e^{-\alpha|e_2(n)-\eta_2(n)|}$$

comparison and decision block use the following algorithm.

(1)

$$\text{IF } |e_1(n) - \eta_1(n)| > |e_2(n) - \eta_2(n)| \text{ THEN}$$
$$\check{s}_1(n) = s_2(n) * \phi_2(n), \check{s}_2(n) = s_2(n) * \phi_2(n)$$

(2)

$$\text{IF } |e_1(n) - \eta_1(n)| < |e_2(n) - \eta_2(n)| \text{ THEN}$$
$$\check{s}_1(n) = s_1(n) * \phi_1(n), \check{s}_2(n) = s_1(n) * \phi_1(n)$$

(3)

$$\text{IF } |e_1(n) - \eta_1(n)| = |e_2(n) - \eta_2(n)| \text{ THEN}$$
$$\check{s}_1(n) = s_1(n) * \phi_1(n), \check{s}_2(n) = s_2(n) * \phi_2(n)$$

3.3. Signal Estimation

In the last block, assuming that the effect of impulsive noise on the data symbols dropped, Maximum likelihood estimation(MLE) reconstruct the transmitter signal. MLE is an optimized detector for digital signals and it do a best estimation of the transmitted data with the least possible number of errors. MLE is a mathematical algorithm to extract useful data out of a noisy data stream. The method of maximum likelihood corresponds to many well-known estimation methods in statistics.

4. SIMULATION RESULTS

We simulate the proposed model with the OFDM modulation and 16QAM constellation under in-home power line channel conditions. For simulate in-home MIMO-PLC, parameters are the same as those given in table I of [30].we set parameters as in Table 1 for the simulation.

Table 1. simulation parameters

Simulation parameter	value
FFT size	64
number of data subcarriers	52
number of bits per OFDM symbol	52
number of OFDM symbols	10^5
modulation	16QAM
SNR	0-20 dB
cyclic prefix(CP)	16

The channel model in Equation (18) can be re-written as:

$$r = hs + n \quad (22)$$

where s is the transmitted signal and h is the corresponding channel coefficient. Channel capacity C_H of the MIMO-PLC channel can be described as [31]:

$$C_H = B.E\{\log_2\left[\det\left(I + \frac{\bar{\gamma}}{n}HH^H\right)\right]\} \quad (23)$$

where E{..}, I, B, $\bar{\gamma}$ and $(..)^H$ are the mathematical expectation, identity matrix, the bandwidth, the average signal-to-noise ratio (SNR) per bit at each receiver branch, and Hermitian transpose. Figure 10 presents a comparison of the BER of the MIMO-OFDM in-home PLC system when the impulsive noise index A is varied(with $\Gamma = 0.01$). In this paper, for modeling impulsive noise, we set A = 0.1 (A = 0.1 is Impulsive noise present in the system in-home plc is simulated).while for a large value of A, the noise channel characteristics approach those of Gaussian noise, for a small value of A, they are similar to those of impulsive noise. Hence, the BER decreases when the value of A increases, as shown in Figure 10.The performance of the simple iterative impulsive noise mitigation algorithms depends on the number of subcarriers in OFDM. in these algorithms, the number of subcarriers plays an important role. for large number of subcarriers, the convergence speed is fast, whereas, for small number of subcarriers, the algorithms converge slowly or event not at all. It was approximated for large number of subcarriers that the multiplication with the FFT matrix converts the impulsive noise channel into AWGN channel. Since for small number of subcarriers, the noise components after FFT has a Class A distribution. The new adaptive iterative method can be repeated with a smaller number of iterations than conventional methods to reduce impulsive noise, and reach to better Performance.

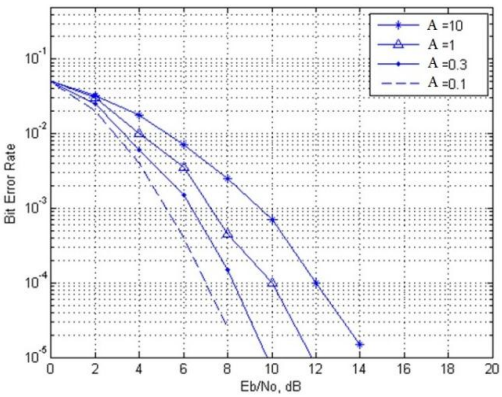

Figure 10. BER Comparison of 2*2 MIMO-OFDM PLC for impulsive noise with $\Gamma = 0.01$ and different values of A.

Figure 11 shows a comparison of the BER performance when the number of iterations is varied. With increasing number of iterations can be achieved better performance of the system.

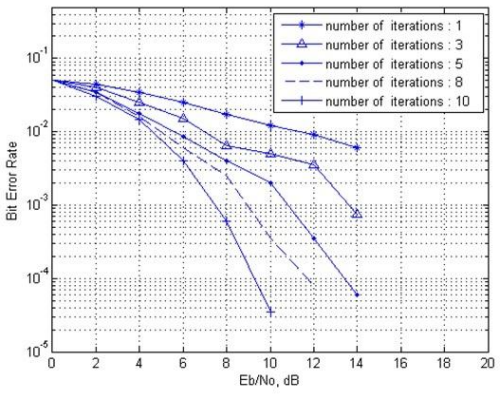

Figure 11. BER Comparison of new iterative method for different of the number of iterations.

Figure 12 shows a comparison of the BER performance between the new iterative method and the conventional method in the in-home MIMO-OFDM systems for impulsive noise and Gaussian noise.

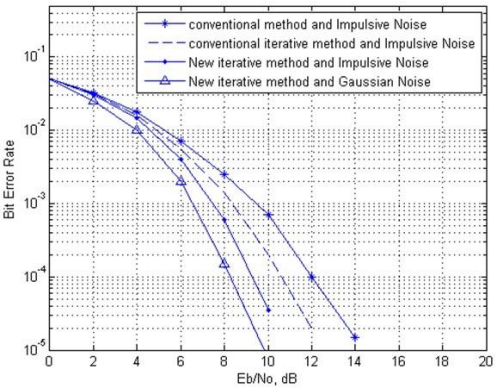

Figure 12. Performance comparison of conventional method with new iterative method.

Figure 13 show a BER Comparison the Known methods, Non linear and Iterative in [32] and Conventional and Iterative in [33] with the method presented in this paper of 2*2 MIMO-OFDM in-home PLC by impulsive noise with A=0.1 and $\Gamma = 0.01$. The proposed method with fewer iterations and Shorter time to reach a better performance than other methods.

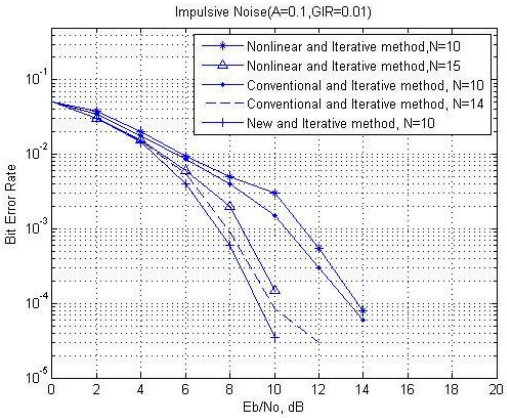

Figure 13. Performance comparison of different method with new method in different values of Iterative.

5. CONCLUSION

In this paper, we proposed an Impulsive Noise Estimation and Suppression in OFDM-MIMO Systems over In-home Power Line Channels. In this method, we use an new iterative method with adaptive technique to recover the signals corrupted by impulsive noise. The proposed method uses impulsive noise detection block, Comparison-Decision block and ML detection block. Adaptive threshold and soft decision are used in the detection and suppression. We evaluated the new iterative method over MIMO-OFDM in-home PLC systems. The computer simulation verified that the proposed scheme was more efficient in the case of both the in-home power channel (MIMO) and the OFDM applications than the methods of the literature. The BER of the reconstructed signal can be decreased by increasing the number of iterations of detection and estimation steps.

6. References

[1] Gardner S. The HomePlug for powerline in home networking. Proc. Int. Symp. Power Line Commun. and Its Appl 2001: 67-72.

[2] Cortes J A, Diez L, Canete F J, Sanchez-Martinez J J. Analysis of the Indoor Broadband Power-Line Noise Scenario. IEEE Trans. Electromagn. Compat 2010; 52. 4: 849-58.

[3] Ghosh M. Analysis of the effect of impulse noise on multicarrier and single carrier QAM systems. IEEE Trans. Commun 1996; 44: 145-147.

[4] Dlhan S, Farka P. Impulsive noise cancellation in systems with OFDM modulation. Journal of Electrical Engineering 2008; 59. 6: 310–16.
[5] Nikookar H, Nathoeni D. Performance evaluation of OFDM transmission over impulsive noisy channels. IEEE. Int. Symp. Personal. Indoor and Mobile Radio Communications 2002; 2: 550 - 4.
[6] Epple U, Shutin D, Schnell M. Mitigation of Impulsive Frequency-Selective Interference in OFDM Based Systems. International Journal of Scientific & Engineering Research 2013; 4. 5: 2253-56.
[7] Ma Y H, So P L, Gunawan E. Performance Analysis of OFDM Systems for Broadband Power Line Communications Under Impulsive Noise and Multipath Effects. IEEE Trans. Power Delivery 2005; 20. 2: 674-82.
[8] Hao L, Guo J. A MIMO-OFDM Scheme over Coupled Multi-conductor Power-Line Communication Channel. IEEE. Int. Symp. Power Line Commun. and Its Appl 2007: 198-203.
[9] Stadelmeier L, Schneider D, Schill D, Schwager A, Speidel J. MIMO for In-home Power Line Communications. in International Conference on Source and Channel Coding (SCC),Ulm, January. 2008.
[10]Canova A, Benvenuto N, Bisaglia P. Receivers for MIMO-PLC channels: Throughput comparison. IEEE. Int. Symp. Power Line Commun. and Its Appl 2010:114-119.
[11] Skolnik M. Introduction to Radar Systems. McGraw-Hill, 2000.
[12] Zimmermann M, Dostert K. An analysis of the broadband noise scenario in powerline networks. IEEE. Int. Symp. Power Line Commun. and Its Appl 2000: 131–8.
[13] Philipps H. Performance measurements of power line channels at high frequencies. IEEE. Int. Symp. Power Line Commun. and Its Appl 1998: 229–37.
[14] Praho B, Tlich M, Pagani P, Zeddam A, Nouvel F. Cognitive detection method of radio frequencies on power line networks. IEEE. Int. Symp. Power Line Commun. and Its Appl 2010.
[15] Esmailian T, Kschischang F R, Gulak P G. In-building power lines as high-speed communication channels: Channel characterization and a test channel ensemble. International Journal of Communication Systems 2003; 16: 381–400.
[16] Al-Bayati A K S, Aloquili O M, AlNabulsi J I. Efficient use of DS/CDMA signals for broadband communications over power lines. International Journal of Communication Systems 2011; 26. 2: 212–21.
[17] Middleton D. Statistical-physical models of electromagnetic interference. IEEE Transactions on Electromagnetic Compatibility 1977;19. 3: 106–27.
[18] Blum R S, Zhang Y, Sadler B M, Kozick R J. Time-domain equalizer for multicarrier systems in impulsive noise. International Journal of Communication Systems 2011; 25. 2:111–20.
[19]Dai H, Poor H V. Advanced signal processing for power line communications. IEEE Communications Magazine 2004; 41. 5:100–07.
[20] Zimmermann M, Dostert K. A multipath model for the powerline channel. IEEE Transactions on Communications 2002; 50. 4: 553–9.
[21] Tonello A M, D'Alessandro S, Lampe L. Bit, tone and cyclic prefix allocation in OFDM with application to in-home PLC. Proc. IEEE IFIP Wireless Days Conference. 2008, p. 23-27.
[22] Tonello A M. Wideband Impulse Modulation and Receiver Algorithms for Multiuser Power Line Communications. EURASIP Journal on Advances in Signal Processing 2007.
[23]Tonello A M. Brief tutorial on the statistical top-down plc channel generator. 2010. [Online].Available: http://www.diegm.uniud.it/tonello/PAPERS/WHITE/TUTORIAL_CHAN_2010.pdf
[24] Clayton R, Paul R. Analysis of Multiconductor Transmission Lines. John Wiley and Sons, Inc, 2004, p. 46-62.
[25] Glover J, Sarma, MOverbye T. Power System Analysis and Design (Fourth Edition). Thomson, 2008 p. 155-213.
[26] Giovaneli C L, Honary B, Farrell P G. Space-frequency coded OFDM system for multi-wire power line communications. IEEE. Int. Symp. Power Line Commun. and Its Appl 2005: 191-5.
[27] Ferreira P. Stability issues in error control coding in the complex field, interpolation, and frame bounds. Signal Processing Letters, IEEE,2000; l. 7. 3: 57–59.
[28] Alamdari M, Modarres-Hashemi M.An improved CFAR detector using wavelet shrinkage in multiple target environments. in 9th International Symposium in Signal Processing and its Applications, 2007. p.1-4.
[29] Zahedpour S, Ferdosizadeh M, Marvasti F, Mohimani G, Babaie-Zadeh M. A novel impulsive noise cancellation based on successive approximations. in Proceedings of SampTa, 2007.
[30] Adebisi B, Ali S, Honary B. Space frequency and space time frequency M3FSK for indoor multiwire communication. IEEE Trans. on Power Delivery 2009; 24. 4: 2361-67.
[31] Versolatto F, Tonello A M. A MIMO PLC Random Channel Generator and Capacity Analysis. ISPLC 2011, p. 66-71.
[32] Chi-Hsiao Yih. Iterative Interference Cancellation for OFDM Signals With Blanking Nonlinearity in Impulsive Noise Channels. IEEE SIGNAL PROCESSING LETTERS 2012; 19. 3: 147-150.
[33] Sukanesh R, Sundaraguru R. Mitigation of Impulse Noise in OFDM Systems. Journal of Information & Computational Science 2011; 8. 12 : 2403–9.